FEASIBILITY OF H₂ PRODUCTION BY ACID CORROSION USING H₂SIF₆ AND WASTE FE SOURCES

Tatiane Carvalho Maeda[a]**, Letícia Teixeira**[a]**, Lorrane Cristine Caixeta**[a]**, Raissa Antonelli**[a,b,] **, Camila Ferreira Pinto**[a]**, Sandra Cristina Dantas**[a,] **, Priscila Pereira Silva**[a]**, Ana Claudia Granato**[a,] **, David Maikel Fernandes**[c,] ** and Geoffroy Roger Pointer Malpass**[a,]*,

[a]Departamento de Engenharia Química, Universidade Federal do Triângulo Mineiro, 38.066-240 Uberaba – MG, Brasil
[b]Faculdade de Engenharia Química, Universidade Estadual de Campinas, 13083-852 Campinas – SP, Brasil
[c]Departamento de Ciências e Linguagens, Instituto Federal de Minas Gerais, Bambuí – MG, Brasil

This study investigated the feasibility of H₂ production by acid corrosion, employing a by-product from the fertilizer industry (Hexafluorsilic acid - H₂SiF₆) and waste iron sources. Different masses of metal from three different sources: iron powder (waste from metal workshops), steel wool and rebar (construction waste), were reacted with various proportions of H₂SiF₆ with HCl. The influence of the variables was evaluated by factorial design, verifying greater production of H₂ for materials with higher contact areas. The lowest production was observed for construction industry waste (rebar) probably due to the presence of protective films and lower contact area. The gas produced was analyzed by gas chromatography and was found to consist only of H₂ (up to 99%) and air. The results indicate a promising application of H₂SiF₆, which is generated in large quantities during phosphate fertilizer production and has few commercial applications. The method proposed is promising, it does not emit toxic or polluting gases, contributing to the sustainable generation of H₂.

Keywords: hexafluorsilic acid; sustainable energy; electrochemical process; corrosion; experimental design; hydrogen gas.

INTRODUCTION

Increasing consumption of energy resources and non-renewable fossil energies, coupled with increased damage to the environment, has led to the pursuit of technologies that aim to produce energy by methods that are clean and sustainable.[1] According to the definition of the United Nations (UN), sustainable development aims at meeting the needs of the present without compromising the ability of future generations to meet their own needs.[2] In this sense, companies have recently adopted practical strategies aimed at corporate social responsibility that balances the relationship between profit, environmental preservation and social actions.[3]

Within this scenario, renewable energy is becoming increasingly accessible, replacing economic dependence on fossil fuels. To accelerate this process, hydrogen gas (H₂) production is a first step. In Europe, for example, H₂ production is based on mainly in steam reform, however this process results in considerable CO₂ emissions.[4]

H₂ is a promising alternative fuel, standing out for its high energy density and low pollution effect. Despite being the most abundant element in the universe, H₂ is present at low concentrations in the atmosphere due to its ability to escape the gravitational pull of the earth. And as a result, it is necessary to develop methods for producing and storing this gas.[5] H₂ is widely used as a raw material in chemical processes such as food production, hydrogenation reactions, ammonia and methanol production and in the pharmaceutical industry, as well as being used to produce renewable energy.[6]

Hydrogen that is produced by green methods can be either stored and used in the chemical industry or used for electricity generation (through fuel cells, for example) with zero post-combustion pollutant.[7] As clean, low-carbon secondary energy, H₂ energy can be applied in renewable energy (mainly wind power and photovoltaic) grid-connected power smoothing, which opens a new way of coupling hydrogen energy storage with renewable energy.[8] Currently, most of the world's H₂ consumption is produced using fossil fuels, but the biggest problem with this method is the generation of CO and CO₂. In addition, conventional methods for producing H₂ require high energy consumption and are not profitable. Thus, this scenario makes it important to search for innovative, sustainable, and economical technologies to produce H₂.[9]

Thus, as hydrogen is not found in the in free form in nature, it is necessary to dissociate it from a primary source, such as hydrocarbons, biomasses or water.[10] Thus, several hydrogen production methods have been studied, as can be seen in Figure 1.[11]

Several studies mention that there exist different methods for hydrogen production such as dark fermentation, coal gasification, electrolysis, amongst other. At present more than 90% of hydrogen in the market is provided by steam reforming of methane.[12,13,14] Electrolysis, for example, is the process in which electrical energy is used to force the non-spontaneous cleavage of H₂O and a large number of variations can be found in the literature.[15] Furthermore, electrochemical hydrogen production via electrolysis provides good energy efficiency as well as with the lowest cost rate. An electrolytic cell is an experimental assembly in which electrolysis is performed, which consists of a pair of electrodes made of a non-reactive metal, such as platinum, immersed in an electrolyte solution. These electrodes must be connected to a power source. In addition, the reaction will easily occur in a 0.1 mol L⁻¹ solution of H₂SO₄, as in this case there are enough ions to conduct electricity.[16] One of the challenges of electrolysis produced from solar technologies is that the transfer of energy from the photovoltaic generator to the electrolyzer is dependent on the instantaneous climatic conditions and how they are connected.[17]

Another method used is anaerobic fermentation, where simple, pure sugars, naturally contained in biomass, are converted into H₂, CO₂ and organic acids in the presence of microorganisms. Among the biological processes for H₂ generation, anaerobic fermentation is considered more viable, as it does not need an external energy source and various types of industrial waste and effluents can be carbon

*e-mail: geoffroy.malpass@uftm.edu.br
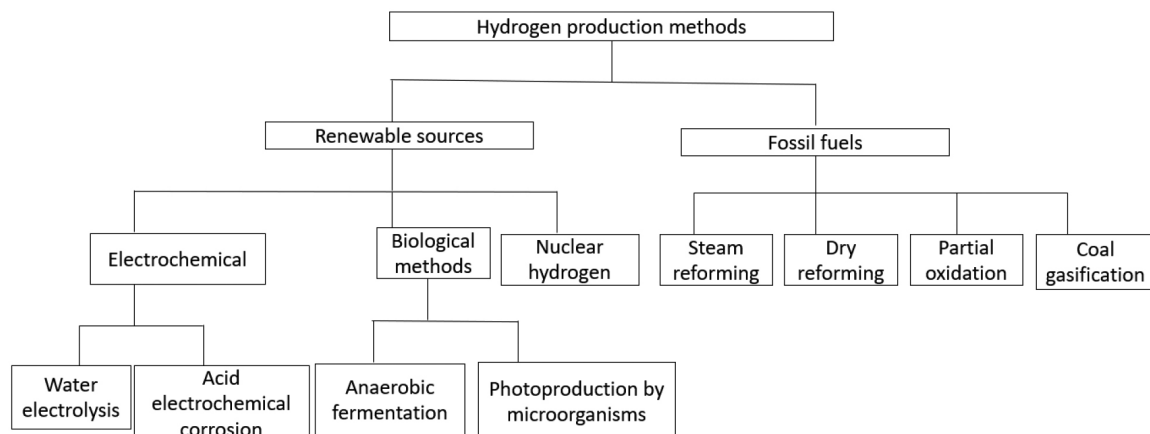
Figure 1. *Examples of types of hydrogen production methods. Adapted from ref. 11*

sources for microorganisms. Large amounts of hydrogen have been produced by this technique. However, the main constraint of this production method is its low performance when compared to other existing chemical and electrochemical methods.[18]

Steam reforming of hydrocarbons is the most widely used process for large-scale H$_2$ production. In this process, a mixture of water vapor and hydrocarbons reacts at high temperatures in the presence of a catalyst, forming a mixture of CO$_2$ and H$_2$. The most used hydrocarbon in the reform process is natural gas (CH$_4$).[19] The main form of H$_2$ generation is by steam reforming furnaces, which are made up of a series of vertical tubes inside an externally heated radiation chamber that focus on the tube walls. Inside these tubes run hydrocarbons or alcohols and water vapor that at high temperatures react endothermically. The problem with this hydrogen production process is that it generates gases that contribute to the greenhouse effect.[20]

Partial oxidation methane of can be complex depending on the catalyst used and the operating conditions. There are two partial oxidation mechanisms: indirect, in which part of the methane is first oxidized to CO$_2$ and H$_2$O, producing synthesis gas.[21] This process has the advantage of being able to dispense the need for catalysts. However, the operating temperature range is 1200-1500 °C range and requires high pressures.[22]

Cyanobacteria use biophotolysis to produce H$_2$ by employing solar energy and water, producing H$_2$ and O$_2$ without emitting CO$_2$, using N$_2$, atmospheric CO$_2$, and H$_2$O as electron sources and sunlight as energy.[23,24] H$_2$ generation by microorganisms has been recognized as being a renewable source, presenting low production costs and not being dependent on agricultural areas, as in the case of biofuels. The production method using photosynthetic microorganisms is a valid alternative, but it is a great challenge, as it presents low efficiencies in the conversion of solar energy, requiring optimization.[25]

An alternative method for the generation of H$_2$, is acid electrochemical corrosion, which can be performed by reusing waste metals from metal workshops or waste building metals. The process takes advantage of the well-known corrosion process of metals to produce H$_2$. Metals display a bright luster when cut/scratched, conduct heat and electricity, furthermore they are malleable and flexible. Metals tend to have low ionization energy, which results in easy cation formation, explaining why they undergo rapid oxidation.[26] Corrosion itself can be defined as the process of material deterioration, most often associated with metals and chemical/electrochemical processes can occur in conjunction with mechanical effects.[27,28]

The electrochemical corrosion method can be used for H$_2$ generation by means of a reaction between acid and metals, which consists in reducing the H$^+$ ion generating H$_2$.[29] The method employs

two half-reactions involving acid (H$^+$) and a metal, and consists in reducing H$^+$ to generate H$_2$, as shown in Equation 1.

$$2H^+ + 2e^- \rightarrow H_2 \tag{1}$$

Generally, this process is spontaneous, involving electron transfer during the oxirreduction process. The reactions involved are shown in Equations 2, 3 and 4.[11]

$$\text{Anode: } Fe \rightarrow Fe^{2+} + 2e^- \tag{2}$$
$$\text{Cathode: } 2H^+ + 2e^- \rightarrow H_2 \tag{3}$$
$$\text{Global reaction: } 2H^+ + Fe \rightarrow Fe^{2+} + H_2 \tag{4}$$
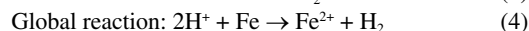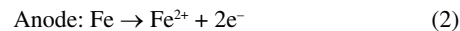
One drawback to this process is the need for concentrated acids, such as HCl, which can increase considerably the cost of the process. One alternative is the use of waste acids that are in need of disposal and one such possibility is Hexafluorsilic acid. Hexafluorsilic acid (H$_2$SiF$_6$), a waste product from the fertilizer industry, is used in water fluoridation, metal surface cleaning/treatment and pH control of textiles and laundries. In addition, FSA is used in the manufacture of aluminum fluoride of low bulk density, cryolite, silicon tetrafluoride and other fluorosilicates.[30] However, there is a large production of this acid requiring new applications. This fact makes the use of this acid in the production of H$_2$ by the acid electrochemical corrosion method an interesting research area.

This study aims to investigate the feasibility of the production of H$_2$ by acid electrochemical corrosion using waste materials (industrial by-products and waste iron). Most importantly, it was intended to employ HCl mixed in different proportions with a by-product of the phosphate fertilizer industry, namely H$_2$SiF$_6$. Additionally, waste metals (iron source) were employed as the substrate for H$_2$ production, and were chosen for their different surface areas. Statistical techniques of experimental design were used to determine the optimal conditions of this process. To the best of our knowledge, this is the first time H$_2$SiF$_6$ has been employed for H$_2$ production.

EXPERIMENTAL

Acid electrochemical corrosion system

The experiments were performed using the system presented in Figure 2, consisting of a batch reactor in which the Fe sample and a solution containing H$_2$SiF$_6$ and HCl are inserted, and the system sealed. The reactor was connected by a hose to the inside of a recipient filled with water and immersed in a water bath. The

subsequent volume of H_2 produced was monitored over time. Various Fe sources were employed: iron powder (waste from metal/welding workshop), steel wool (n° 2) and rebar (construction waste). As the gas was produced, pressure was exerted on the water inside the water bath and the displaced water level was equivalent to the volume of gas produced.
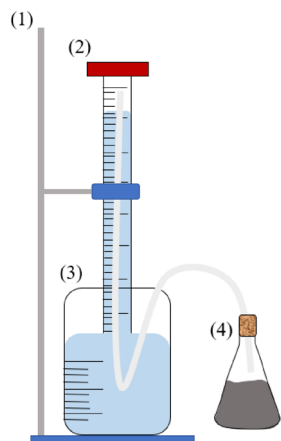
Figure 2. *Hydrogen production system consisting of (1) universal holder, (2) measuring column filled with water for H_2 collection, (3) water bath and (4) sealed batch reactor containing (H_2SiF_6 + HCl + Fe)*

Factorial design

Adequate experimental design requires that the experiment provides the required information. It is necessary to quantitatively evaluate the influence on the response variables and the interactions between the factors. For this, a complete factorial design can be used, which permits the elaboration of a minimum of experiments, improving the quality of the information obtained.[13]

Data were analyzed through a factorial design 3^3 (three levels and three variables) for each material. The experimental matrix was generated by the Statistica® software (license from PMPIT - ICTE - UFTM). The independent variables analyzed were mass (X_1), volumetric acid fraction (H_2SiF_6/HCl) – When the acid fraction tends to 1, H2SiF6 is present at 100% – (X_2) and time (X_3), being the volume of gas obtained the response variable. The coded levels

and actual values of each variable are presented in Table 1. Assays were performed in triplicate.

Table 1. Variables studied with coded and real values for the different iron samples

IRON POWDER			
Factors	Level		
	-1	0	+1
Mass (g)	5	10	15
Volumetric acid fraction (v/v)	0.3	0.6	0.9
Time (s)	120	480	840
STEEL WOOL			
Factors	Level		
	-1	0	+1
Mass (g)	0.1	0.5	1.5
Volumetric acid fraction (v/v)	0.1	0.5	0.9
Time (s)	240	600	720
REBAR			
Factors	Level		
	-1	0	+1
Mass (g)	10	15	20
Volumetric acid fraction (v/v)	0.3	0.6	0.9
Time (s)	780	2820	4860

Orthogonal central composite design

The tests of the orthogonal central composite design (OCCD) were performed to find the optimal condition of the H_2 production process for each material analyzed, based on the results obtained during the factorial design. Table 2 displays the levels of each variable studied for OCCD.

In the case of iron powder, the mass was kept constant at 25 g. For steel wool n° 2, the time was kept constant at 10 minutes due to system limitations such as the size of the beaker available in the laboratory. In the case of rebar, all variables were significant.

Gas Chromatography

To qualitatively analyze gas produced, the technique of gas chromatography was employed. The samples were collected for

Table 2. Variables studied for the OCCD coded and real values for the different iron samples

IRON POWDER					
Factors	Level				
	-α	-1	0	+1	- α
Volumetric acid fraction (v/v)	0.23	0.3	0.6	0.9	0.96
Time (min)	0,74	2	8	14	15,26
STEEL WOOL					
Factors	Level				
	- α	-1	0	+1	- α
Mass (g)	0.895	1.0	1.5	2.0	2.105
Volumetric acid fraction (v/v)	0.458	0.5	0.7	0.9	0.942
REBAR					
Factors	Level				
	- α	-1	0	+1	- α
Mass (g)	5.50	20	55	90	104.49
Volumetric acid fraction (v/v)	0.196	0.3	0.55	0.8	0.903
Time (min)	11,72	20	40	60	68,28

analysis at the optimized condition, after the factorial design and OCCD. For this purpose, the gas stream generated was collected in a syringe and transferred was stored in gasometric ampoules. The gas stream generated during the treatment were analyzed for each of the materials using a gas chromatograph (Shimadzu GC-2014), equipped with a thermal conductivity detector and a Carboxen 1010 Plot column.

RESULTS AND DISCUSSION

Factorial design

Iron powder

Table 3 presents the values obtained for the parameter p, as well as the values of the coefficients and the accumulated square error for iron powder (R^2 of 0.9654). For a more refined analysis, the statistically non-significant terms were eliminated, with the quadratic term of mass (X_1^2) and quadratic time (X_3^2) being removed.

Table 3. Regression relations for iron powder monitored in the factorial design 3^3

Factor	p	Coefficient	Cumulative Square Error
Mean	0.00	137.14	8.67
(X_1) Mass	0.00	36.78	12.27
(X_2) Volumetric acid fraction	0.00	114.11	24.54
(X_2^2)	0.00	-32.89	21.25
(X_3) Time	0.00	89.00	12.27
(X_1X_2)	0.00	36.92	15.03
(X_1X_3)	0.00	25.42	15.03
(X_2X_3)	0.00	60.08	15.03

Eq. 5 represents the model obtained and Figure 3A presents the verification of the model fit. From Figure 3A it can be observed that

the model given in Eq. 5 is adequate to describe the observed results as the observed values follow closely the tendency given in Eq. 5.

$$V = 137.14 + 36.78X_1 + 114.11X_2 - 32.89X_2^2 + 89X_3 + 36.92X_1X_2 + 25.42X_1X_3 + 60.08X_2X_3 \quad (5)$$

From the Pareto graph (Figure 3B) it can be observed that time (X_3) was the most significant variable, followed by acid fraction (X_2), the interaction between the acid fraction and time (X_2X_3) and mass (X_1). From the residuals plot (Figure 3C) it can be seen that the model is adequate, with points distributed randomly around zero, indicating that there was no bias in the results. The response surfaces are given in Figures 4A-C.

From Figure 4A, it can be noted that the increase in acid fraction leads to an increase in gas production, but the increase in mass is not a significant factor. The influence of the acid fraction on gas production indicates that HFSA can substitute HCl and improve the rate of reaction and, importantly reduce the cost of the process. Figure 4B demonstrates that yield increases linearly with increasing mass and time of reaction, indicating that some form of inhibition is overcome at exposure longer times. From Figure 4C the interaction between fraction and time increases the production, in which both the linear time and the linear fraction are very significant, as well as the interaction between them. This phenomenon is well-known, and the increase of hydrogen production can be related with anodic polarization process and/or during anodic polarization the 'background' corrosion current increases and therefore more hydrogen evolution is observed. This background corrosion current would be associated with the decrease of partially protective oxide film (anodic event) that results in an enhanced auto-catalytic cathodic activity for hydrogen evolution.[31-33]

Steel wool n° 2

Table 4 presents the values of p, coefficient, and accumulated error for steel wool n° 2. Several terms were eliminated (such as X_1^2 (quadratic mass), X_3^2 (quadratic time), $X_1^2X_2^2$ (interaction between

(A)

(B)

(C)
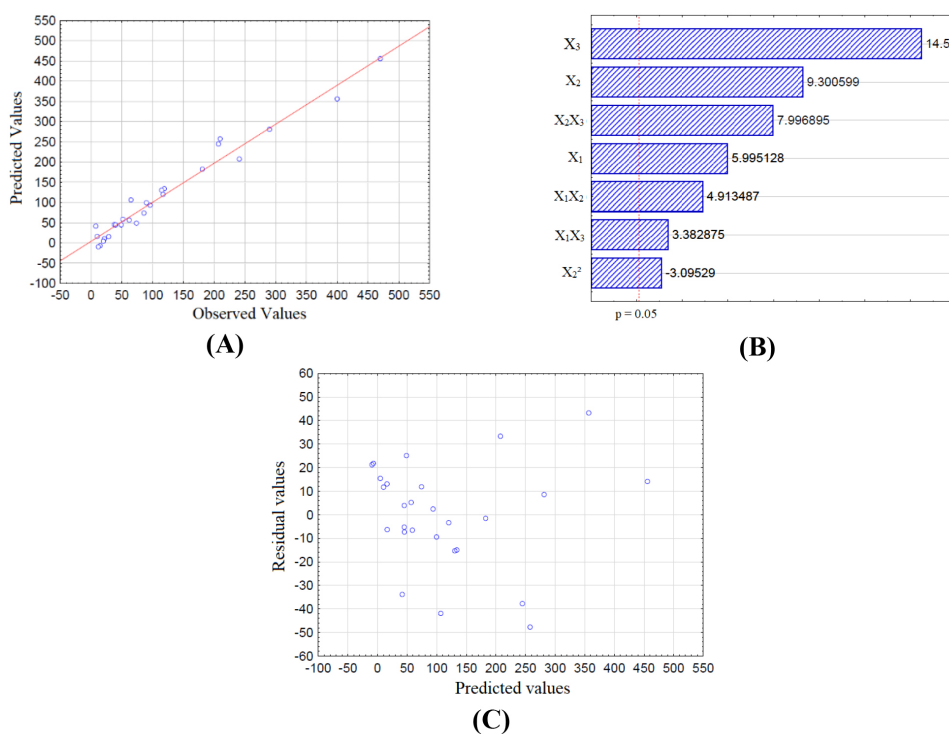
Figure 3. *(A) - Predicted versus observed values for iron powder; (B) - Pareto graph for iron powder; (C) - Graph of residues for iron powder*
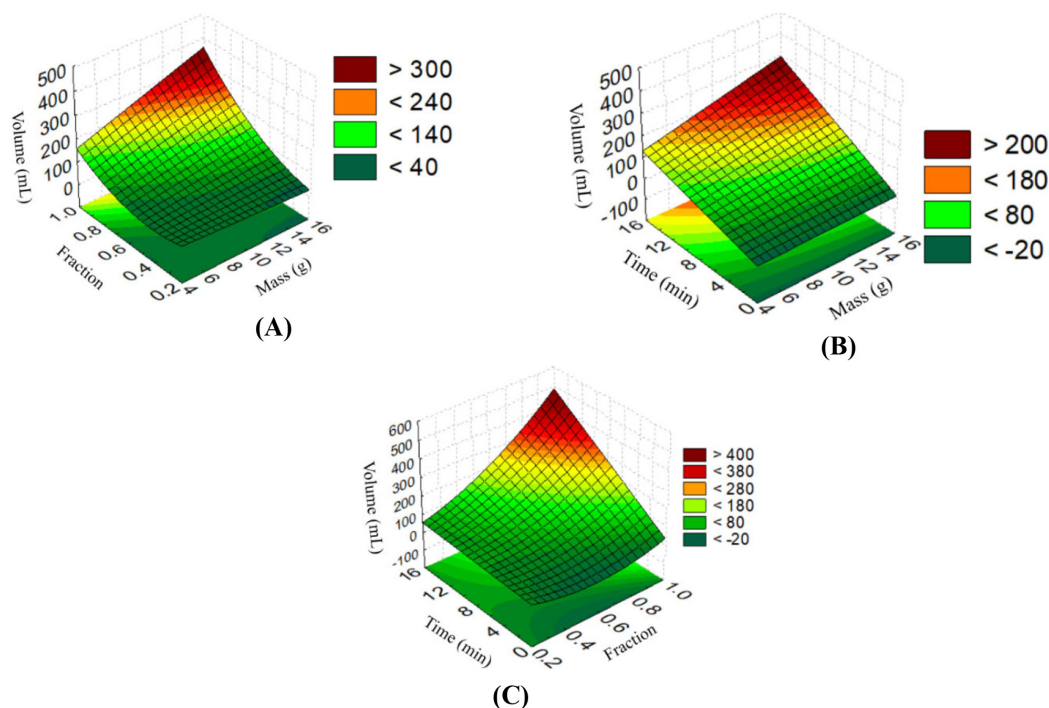
Figure 4. *Response surfaces for iron powder between (**A**) fraction and mass, (**B**) mass and time, and (**C**) fraction and time*

Table 4. Regressions obtained for steel wool monitored during the factorial design 3^3

Factor	p	Coefficient	Cumulative Square Error
Mean	0.00	105.11	1.32
(X_1) Mass	0.00	52.00	1.62
(X_2) Volumetric acid fraction	0.00	38.06	1.62
(X_2^2)	0.02	3.58	1.40
(X_3) Time	0.00	47.28	1.62
(X_1X_2)	0.00	17.08	1.98
($X_1X_2^2$)	0.00	9.87	1.72
($X_1^2X_2$)	0.00	5.71	1.72
(X_1X_3)	0.00	21.08	1.98
(X_2X_3)	0.00	18.25	1.98

quadratic mass and quadratic fraction), $X_1^2X_3$ (interaction between mass quadratic and time), $X_1X_3^2$ (mass and quadratic time), $X_1^2X_3^2$ (quadratic mass and quadratic time), $X_2^2X_3$ (quadratic fraction and time), $X_2^2X_3^2$ (quadratic fraction and quadratic time), and $X_2X_3^2$ (fraction and quadratic time)), as they did not present significance at the 95% confidence interval. The model is given in Eq. 6 ($R^2 = 0.9939$) and the relevant predicted vs. observed values are given in Figure 1S A and the model is adequate to describe the observed results for H_2 production from Fe powder.

$$V = 105.11 + 52X_1 + 38.06X_2 + 3.58X_2^2 + 47.28X_3 + 17.08X_1X_2 + 9.88X_1X_2^2 + 5.71X_1^2X_2 + 21.08X_1X_3 + 18.25X_2X_3 \quad (6)$$

From the Pareto graph (Figure 5) it can be verified that the linear terms of mass (X_1), fraction (X_2) and time (X_3) were significant in the confidence interval analyzed. The interactions X_1X_3 (mass/time), X_2X_3 (acid fraction/time) and X_1X_2 (mass/acid fraction) were also significant, as was the quadratic term of fraction (X_2^2). From the plot of the residuals (Figure 1S B) it can be verified that the points are
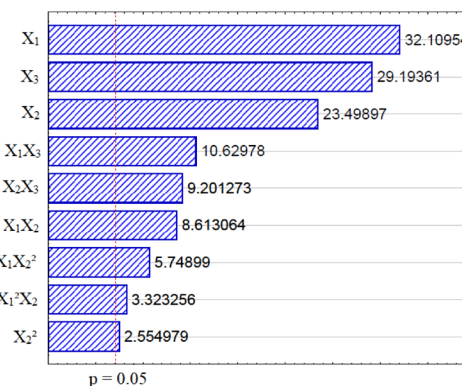
Figure 5. *Pareto graph for steel wool*

grouped randomly around zero, meaning there was no trend, and the model is adequate to the data.

The response surfaces for the factorial design for gas production from the steel wool, are given in Figure 6A-C. From Figure 6A, it is observed that for a small and constant mass the fraction has a low influence on the volume of gas produced, as the volume produced for a low fraction is almost the same as when the fraction is high. Therefore, when a lower mass is used, there is no reason to use higher acid fractions.

When increasing the mass, it is observed that higher fractions increase the volume of gas produced. However, when analyzing the effect of the fraction for a mass of 1.6 g, it is observed that the production tends to stabilize close to an acid fraction of 1.0. This which may indicate that the acid fraction can consume all the steel wool present or that some form of passivating film is formed.[32] From the analysis of Figure 6B, linearity observed in the variation of the terms mass and time. For smaller masses it would take longer to obtain appreciable gas production, while for larger mass quantities the time required would be shorter. Therefore, it would not be interesting to employ large amounts of mass if there was not a sufficiently long time for the reaction occur, nor would it be efficient to provide a long time if the steel wool mass is too low. From Figure 6C (time vs acid fraction),
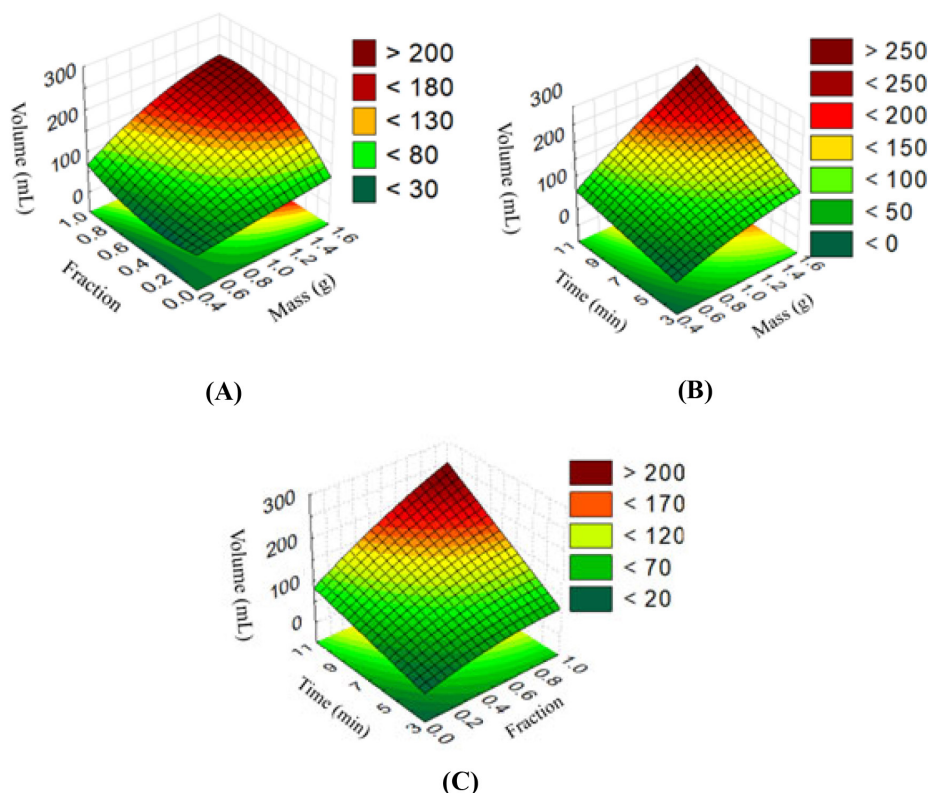
Figure 6. *Response surfaces for steel wool between (A) fraction and mass, (B) mass and time, and (C) fraction and time*

it can be observed that time behaves approximately linearly for both low and high fractions. It is noted that for a short time, the increase of the acid fraction results in a small influence on the increase of the volume of gas produced. For a longer time interval, larger acid fractions provide greater volumes of gas. Thus, the increase in the experimental time would be justified only if accompanied by an increase in the acid fraction, requiring longer times and higher fractions for better results. The quantity of hydrogen produced is related to chemical composition of the sample (e.g., type of valence state of iron – Fe, Fe^{2+}, or Fe^{3+}) and the quantity of iron present. Using 20.76 (%wt.) of steel wool a theoretical total of 31.50 mL g^{-1} can be produced and 40.35 mL g^{-1} if 24.15 (%wt.) is employed. Thus, the mass increase is related to the greater quantity of hydrogen produced, as seen in the literature.[34]

Rebar

In the case of rebar, the analysis of p values resulted in the elimination of a number of terms (X_3^2, $X_1^2X_2$, $X_1^2X_2^2$, $X_1X_3^2$, $X_1^2X_3^2$, X_2X_3, $X_2X_3^2$ and $X_2^2X_3^2$). The regression relations are given in Table 5, where linear term of acid fraction (X_2) was not disregarded from the model, as this would considerably decrease the value of R². The model, represented by Eq. 7, displayed a reasonable fit to the data (Figure 2S A) with R² of 0.9930.

$$V = 79.11 + 27.24X_1 - 6.21X12 + 6.11X_2 + 10.08X_2^2 + 60.96X_3 + 4.50X_1X_2^2 + 26.96X_1X_3 - 4.02X_1^2X_3 + 13.59X_2^2X_3 \quad (7)$$

From the Pareto graph (Figure 7) it was observed that the linear term of time (X_3) is significant compared to the other terms evaluated, having with a positive influence on the response. From the residuals graph (Figure 2S B) it was observed that the points are situated randomly around zero, which proves that the model is appropriate for the data, as no trend is observed.

The response surfaces are given in Figure 8A-C. From Figure 8A it was found that the increase in mass has the effect of increasing

Table 5. Regression relations obtained for rebar monitored in the factorial design 3³

Fator	p	Coefficient	Cumulative Square Error
Mean	0.00	79.11	2.47
(X_1) Mass	0.00	27.24	6.28
(X_1^2)	0.00	-6.21	5.06
(X_2) Acid fraction	**0.09**	**6.11**	**6.48**
(X_2^2)	0.00	10.08	5.79
(X_3) Time	0.00	60.96	6.28
($X_1X_2^2$)	0.05	4.50	7.19
(X_1X_3)	0.00	26.96	4.49
($X_1^2X_3$)	0.05	-4.02	3.59
($X_2^2X_3$)	0.00	13.59	7.19
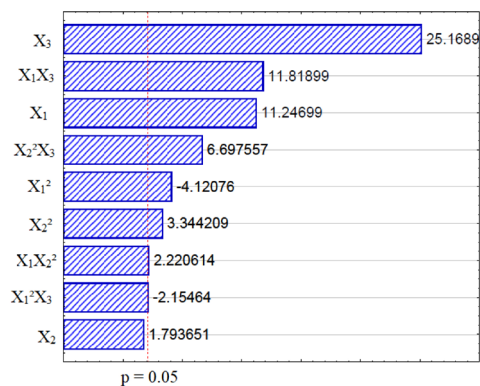
Figure 7. *Pareto graph for rebar*

production, indicating that the larger the mass, the greater the production. However, increasing both acid fraction and mass does not significantly increase yield, a fact that can be confirmed in Table 5 for

X_1X_2 (mass/acid fraction), showing that the interaction between linear mass and linear acid fraction is not significant. From Figure 8B, it can be observed that the longer the time, the greater the production. The increase in mass and time result in an increase in the volume of gas obtained, which confirms the result observed in the Pareto graph (Figure 8B), where the X_1X_3 (mass/time) interaction has significance at the 95% confidence interval with positive influence.

In Figure 8C it was observed that for smaller values of time with the increase of the acid fraction the production decreases. However, it was found that the longer the time and the fraction the greater the gas production. This can be verified in the experiments with fractions of 0.6 and 0.9, which did not initially present large production differences, as the acid fraction increase was not relevant. However, over time, it was verified that the 0.9 fraction had a production higher than the 0.6. This may be related to the reaction kinetics being slower initially due to the presence of oxides or other barrier products that are removed at longer exposure times, as expected in a corrosion process.[33]

Orthogonal central composite design

Based on the factorial design, analyses were performed to obtain the optimal point for each material through the orthogonal central composite design (OCCD).

Iron powder
Table 6 presents the regression relations obtained in the OCCD for iron powder. Table 6 demonstrates that only the quadratic term of time (X_3^2) was not significant in the confidence interval analyzed. Eq. 8 represents the model obtained ($R^2 = 0.9835$) and the model (fit and randomness) can be verified in Figure 3S A and 3S B.

$$V = 287.55 + 234.47X_3 - 40.51X_3^2 + 343.38X_2 + 162.54X_2^2 + 220.00X_3X_2 \quad (8)$$

Table 6. Regression relations obtained for iron powder monitored in the OCCD

Factor	p	Coefficient	Cumulative Square Error
Mean	0.00	287.55	31.69
(X_3) Time	0.00	234.47	49.24
(X_3^2)	**0.24**	**-40.51**	**62.60**
(X_2) acid fraction	0.00	343.38	49.14
(X_2^2)	0.00	162.54	62.17
(X_2X_3)	0.00	220.00	64.81

From the Pareto graph (Figure 9A), the linear term of the acid fraction (X_2) was the most significant. The terms X_3 (time), X_2X_3 (interaction between fraction and time) and X_2^2 (quadratic fraction) were also significant. The quadratic term of time (X_3^2) was not significant ($p > 0.05$). However, this variable was not eliminated from the model, as the value of R^2 decreased considerably, reducing the reliability of the adjustment.

By analyzing the response surface of the fraction over time, Figure 9B shows that the increase of these variables has a positive influence on the response. Table 7 was also obtained, with the maximum observed and minimum observed points and the critical point calculated by the software.

Table 7. Observed minimum and maximum values and critical point obtained by OCCD for iron powder

Factor	Minimum observed	Critical value	Maximum observed
Time	0.74	8.03	15.26
Fraction	0.23	0.28	0.96

The critical value provided was expected to be the optimal process point, however, the critical value presented is a cell point and not the

(A)

(B)

(C)
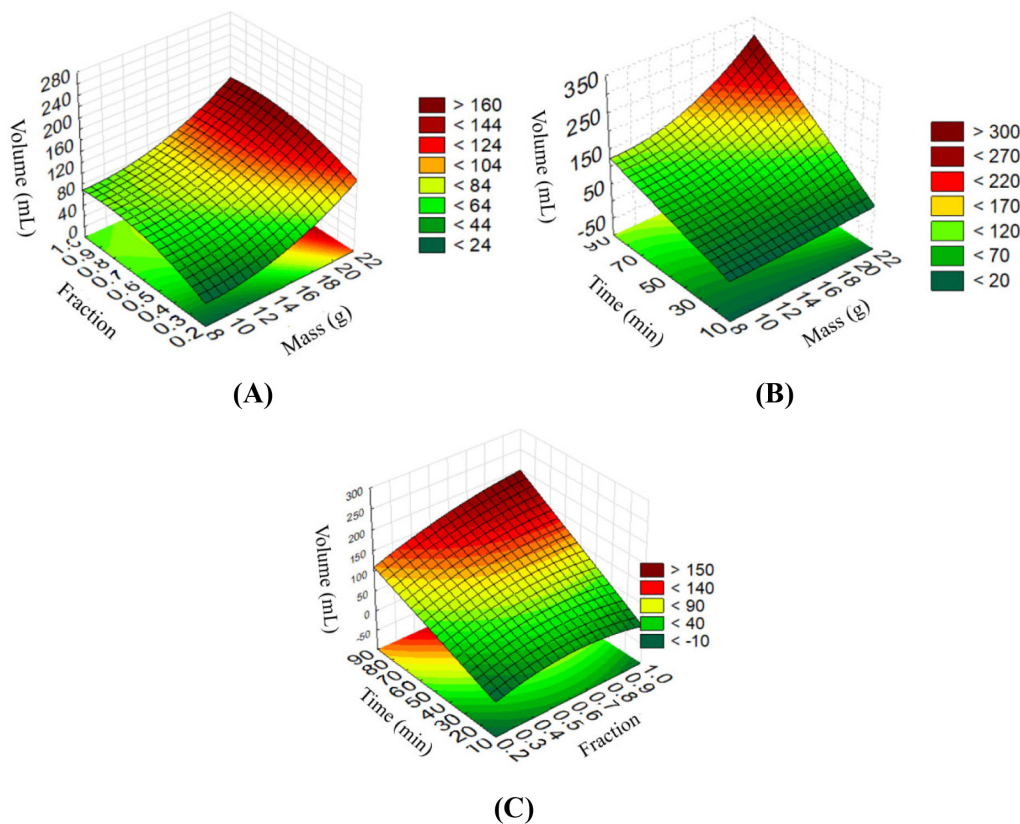
Figure 8. *Response surfaces for rebar between (**A**) acid fraction and mass, (**B**) mass and time, and (**C**) fraction and time*

(A)

(B)
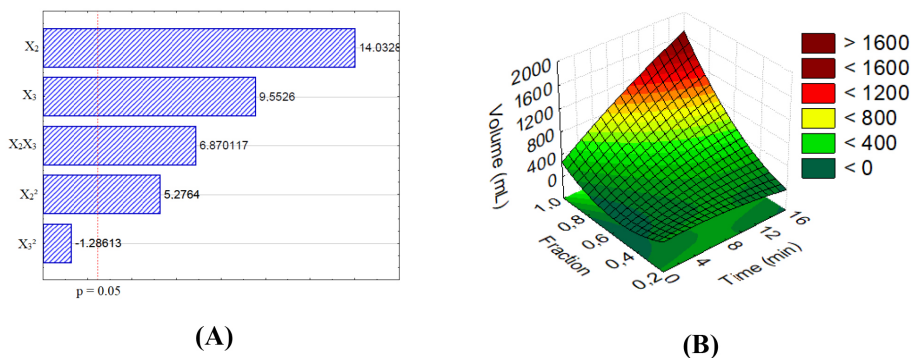
Figure 9. *Results for OCCD experimental design with iron powder: (A) Pareto graph, and (B) response surface for acid fraction vs. mass*

highest production point. Thus, due to the physical limitations of the experiment, the maximum gas production point for the process is the maximum value observed with the fraction of 0.96 and time of 15.26 minutes. The oxidation of iron and by consequence the H_2 production can be decreased due to characteristics of the waste (such as the presence of inhibitors or contaminants metals), however this parameter was not evaluated in present study.[35]

Steel wool n°2

Table 8 presents the values of P, coefficient, and accumulated error for steel wool. The interaction of X_1 (mass) and X_2 (acid fraction) was not significant even though a positive response was observed. However, the effects of X_1^2 (quadratic mass), X_2^2 (quadratic fraction) and X_1X_2 (mass and fraction) were maintained in the model.

Table 8. Regression relations obtained for steel wool monitored in the OCCD

Factor	p	Coefficient	Cumulative Square Error
Mean	0.00	224.08	10.00
(X_1) Mass	0.00	84.41	7.78
(X_1^2)	**0.57**	**-5.95**	**9.89**
(X_2) acid fraction	0.00	35.82	7.78
(X_2^2)	**0.09**	**-19.61**	**9.89**
(X_2X_3)	**0.16**	**16.25**	**10.23**

The model obtained for OCCD of the steel wool the presented an R² of 0.9605 and the equation that represents it can be seen in Eq. 9 and the fit and randomness are given in Figure 4S A and 4S B, respectively.

$$V = 224.08 + 84.41X_1 - 5.95X_1^2 + 35.82X_2 - 19.61X_2^2 + 16.25X_2X_3 \qquad (9)$$
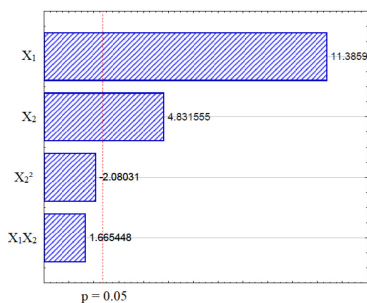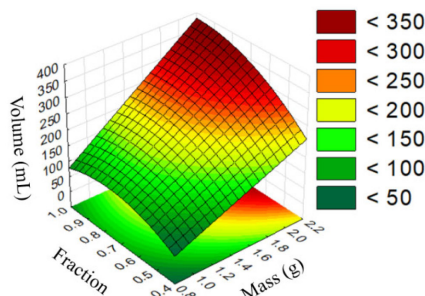
From the Pareto graph (Figure 10A) the linear mass (X_1) was the most significant variable. The linear fraction (X_2) was also significant. However, the quadratic term of fraction (X_2^2) had a negative effect, just as the interaction between linear mass and linear fraction (X_1X_2) was not significant, a fact that can be observed in Table 7 ($p > 0.05$).

The response surface (Figure 10B) demonstrates that the mass increase has a linear effect, causing gas production to increase, confirming the significant influence of mass. Moreover, when a high mass is analyzed, it is observed that regardless of the fraction, the yield was adequate, and that the fraction increase tends to stabilize, as the curve seems to approach a maximum point. This fact may have occurred due to total consumption of the mass when a high fraction is employed, as suggested for the iron powder. Table 9 presents the critical value as well as the observed minimum and maximum values. The values presented in Table 9 demonstrate that the critical point is not physically possible, since the fraction 2.47 cannot exist since it must be < 1. In addition, the mass of 11.12 g would not fit within the equipment used. This occurred because the software used is statistical and thus the statistical parameters should be disregarded. Thus, the maximum yield would occur using a fraction of 0.94 and mass of 2.10 g.

Table 9. Observed minimum and maximum values and critical point obtained by OCCD for steel wool

Factor	Minimum observed	Critical value	Maximum observed
Mass	0.89	11.12	2.10
Fraction	0.46	2.47	0.94

Rebar

Regression ratios obtained for rebar are given in Table 10. The terms of the interactions of the mass and acid fraction (X_1X_2) and acid fraction and time (X_2X_3) were eliminated, and the quadratic fraction (X_1^2) and the quadratic time were not disregarded from the model, as

(A)

(B)

Figure 10. *Results for OCCD experimental design with steel wool: (A) Pareto graph, and (B) response surface for acid fraction vs. mass*

Table 10. Regression relations obtained for rebar monitored in the OCCD

Factor	p	Coefficient	Cumulative Square Error
Mean	**0.44**	**9.98**	**12.55**
(X_1) Mass	0.01	23.69	15.37
(X_1^2)	**0.60**	**5.06**	**18.83**
(X_2) acid fraction	0.01	24.00	15.37
(X_2^2)	0.00	29.99	18.82
(X_3) Time	0.00	26.73	15.37
(X_3^2)	**0.44**	**7.49**	**18.82**
(X_1X_3)	0.04	22.50	18.82

this would decrease the value of R^2. Eq. 10 represents the obtained model, with R^2 of 0.828 and the relevant predicted vs. observed values are given in Figure 5S A and the model is adequate to describe the observed results for H_2 production from rebar.

$$V = 9.98 + 23.69X_1 + 5.06X_1^2 + 24.00X_2 + 29.99X_2^2 + 26.73X_3 + 7.49X_3^2 + 22.50X_1X_3 \quad (10)$$

From the Pareto graph obtained (Figure 11A) it can be observed that the linear term of time is more significant. Quadratic fraction (X_2^2), linear mass (X_1), linear fraction (X_2) and the interaction between linear fraction and linear time (X_2X_3) are also quite significant. However, the quadratic time and quadratic mass in the 95% confidence interval were not significant. From the residuals graph (Figure 5S B) it was observed that the points are situated randomly around zero, which proves that the model is appropriate for the data, as no trend is observed.

The response surface (Figure 11B) of the mass and time interaction presents that an increase in mass and time resulted in exponential behavior in gas production, so that the interaction of both would lead to maximum production. The maximum and minimum points observed and the critical point are presented in (Table 11).

The critical value at which an optimal production point would be obtained, but the critical value is a cell point. Therefore, as the fraction

Table 11. Observed minimum and maximum values and critical point obtained by OCCD for rebar

Factor	Minimum observed	Critical value	Maximum observed
Mass	5.50	40.99	104.49
Fraction	0.19	0.37	0.90
Time	11.72	25.19	68.28
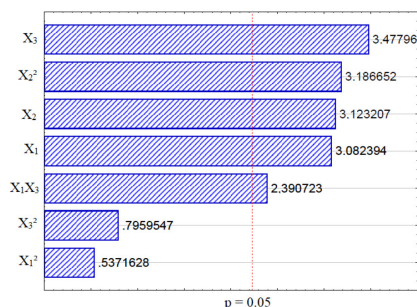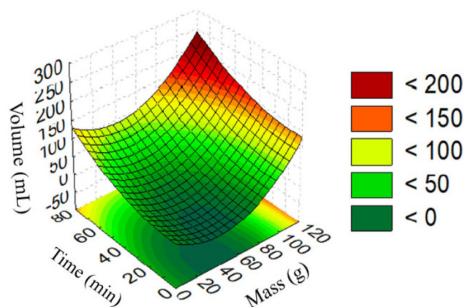
must be less than 1, and there is a limitation for mass, the maximum yield occurs for a fraction of 0.90, mass of 104.49 and a time of 68,28 min. Rebar was the material that produced the least amount of gas due to its lower contact surface, as would be expected.[31] Additionally, oxide film formation may have occurred, which would function as a protective layer on the metal surface. Rebar oxidation products include iron oxides (Fe_2O_3, Fe_3O_4), iron sulfides (FeS) and others such as iron sulfate ($Fe_2(SO_4)_3(H2O)_Z$) and these substances can form a surface film that can cause a decrease in hydrogen production.[33,36]

Gas Chromatography

The gases produced were tested at the optimum condition for H_2 production obtained in the OCCD. When analyzing the gas produced using gas chromatography, the presence of H_2 (up to 99%) and only traces of air were observed for all the gas samples. No other reaction product was observed indicating that the process produces hydrogen with high purity. The presence of air in the analysis may be due to the methodology used for the injection. Thus, there was no evidence of unwanted reactions taking place in the reaction system.

Comparison

Table 12 presents the quantities of gas produced and an estimate of the cost of the production price considering the volume of HCl used. In Table 12 it can be seen that the iron powder, due to its extensive contact area, produces large volumes of hydrogen gas, reaching 2770 mL, when the volumetric fraction of H_2SiF_6/HCl is equal to 0.9, with time at 30 min and 25 g of iron powder employed. For steel wool, it is observed that a maximum of 330 mL of H_2 is produced, with an acid fraction of 0.9, at 10 min and 2 g of iron wool, lower than that obtained from iron powder. Rebar, on the other hand, needs larger masses and prolonged times (90 g and 60 min), respectively, to produce a volume of 160 mL This confirms that future application of the acid corrosion process should be applied to materials of greater contact area or after an initial treatment step.

Additionally, Table 12 indicates the relationship between H_2 produced in terms of iron mass used and time spent in minutes over the time obtained in the OCCD. It is also possible to observe the value in reais and in dollars of the cost based on the HCl (U\$ 11.25 per L) spent in the process in which there was maximum H_2 production. The cost of HCl was used as an indicator as all the remaining materials were obtained by donation. Thus, the cost analysis shows that to produce 1 L of H_2, the cost is lower if using iron powder (US\$ 0.02 L^{-1}), while using rebar the production cost is higher (U\$ 0.70 L^{-1})) This indicates that the larger the contact surface, the greater the production of hydrogen, as well as the greater use of reagents.

However, additional results produced by this laboratory demonstrate that it is possible to use an alternative chloride ion source, that is cheaper

(A)

(B)

Figure 11. *Results for OCCD experimental design with rebar: (A) Pareto graph, and (B) response surface for acid fraction vs. mass*

Table 12. Comparison of maximum hydrogen production and price for each of the studied materials

Materials	Maximum H$_2$ production (mL)	Gas produced per mass (mL g^{-1})	Gas produced per mass (mL g^{-1} min^{-1})	Cost (US$ L^{-1} H$_2$)[#]	Cost in R$ (R$ L^{-1} H$_2$)
Iron powder	2770	110.8	3.69[1]	0.02	0.11
Steel wool	330	165.0	16.50[2]	0.17	0.91
Rebar	160	1.8	0.03[3]	0.70	3.75

[#]Exchange rate 05/05/2021 (1US$= R$5.35). [1]30 min; [2]10 min; [3]60 min.

and safer than HCl, and achieve the same gas productivity and reduce the cost per liter of hydrogen produced by up to 95.3 %, when compared to the system using only HCl as a corrosive solution.[37]

CONCLUSIONS

The present study demonstrates that it is feasible to employ a by-product of the fertilizer industry to produce H$_2$ from waste iron sources. It was observed that iron sources with larger contact areas produced greater volumes of H$_2$, as would be expected. Iron powder from iron workshops resulted in the highest gas production, followed by steel wool. Rebar was the material that produced the smallest amount due to its smaller contact area and the difficulty of corrosion, since oxide formation may have occurred, which functioned as a protective film on the metal surface. This indicates that preprocessing of certain types of waste (for example grinding) may be required.

The tests indicated promising application of mixtures of H$_2$SiF$_6$ and HCl for accelerated acid corrosion, providing added value for industrial by-products and waste metals. The method has been shown to be efficient, does not emit any toxic or polluting gas and is economically viable, thus contributing to H$_2$ generation technologies. Future studies will concentrate on the scale-up of the process for future applications.

SUPPLEMENTARY MATERIAL

Factorial design plots (Figures 1S–5S) are freely available at http://quimicanova.sbq.org.br, in PDF format.

ACKNOWLEDGMENTS

REFERENCES

1. Dubent, S.; Mazard, A.; *Int. J. Hydrogen Energy* **2019**, *44*, 15622.
2. https://academicimpact.un.org/content/sustainability#:~:text=In%20 1987%2C%20the%20United%20Nations,development%20 needs%2C%20but%20with%20the, accessed in June 2021.
3. https://www.wwf.org.br/participe/porque_participar/sustentabilidade/, accessed in June 2021.
4. https://www.iea.org/newsroom/news/2018/may/commentar-offshore-wind-and hydrogen-for-industry-in-europe.html, accessed in June 2021.
5. Lee, J. D.; *Química inorgânica não tão concisa*, 5ª ed, Blucher: São Paulo, 1999.
6. Alves, H. J.; Bley Junior, C.; Niklevicz, R. R.; Frigo, E. P.; Frigo, M. S.; Coimbra-Araújo, C. H.; *Int. J. Hydrogen Energy* **2013**, *38*, 5215.
7. Sapountzi, F. M.; Gracia, J. M.; Weststrate, K.; Hans, O. A.; Fredriksson, J. W./ Niemantsverdriet, H.; *Prog. Energy Combust. Sci.* **2017**, *58*, 1.
8. Kong, L.; Li, L.; Liu, C.; Ma, P.; Bian, Y.; Ma, T.; *Int. J. Hydrogen Energy* **2021**, *46*, 2847.
9. Martínez-Salazar, A. L.; Melo-Banda, J. A.; Coronel-García, M. A.; González-Barbosa, J. J.; Domínguez-Esquivel, J. M.; *Renewable Energy* **2020**, *146*, 2517.
10. Medeiros, W. B.; Botton, J. P.; *Anais do II Encontro de Iniciação Científica da Unila,* Foz do Iguaçu, Brasil, 2013.
11. Kumar S. S.; Himabindu V.; *Mater. Sci. Energ. Technol.* **2019**, *2*, 442.
12. Chozhavendhan, S.; Rajamehala, M.; Karthigadevi, G.; Praveenkumar, R.; Bharathiraja B.; *Case Studies in Chemical and Environmental Engineering* **2020**, *2*, 100038.
13. Dincer, I.; Acar, C.; *Int. J. Hydrogen Energy* **2015**, *40*, 11094.
14. Acar, C.; Dincer, I.; *J. Cleaner Prod.* **2019**, *218*, 835.
15. Haussinger, P.; Lohmuller, R.; Watson, A. M. In *Ullmann's Encyclopedia of Industrial Chemistry*, Wiley VCH: Weinheim, 2007, pp. 1-155.
16. Chang, R.; *Química Geral: conceitos essenciais*, 4ª ed., Bookman Editora Ltda: Porto Alegre, 1988.
17. Knob, D.; Silva, A. M. S.; Masters Dissertation, Universidade de São Paulo, Brasil, 2013.
18. Soares, J. F.; PhD Thesis, Universidade Federal Rural de Santa Maria, Brasil, 2019.
19. Cruz, F. E.; Masters Dissertation, Universidade de São Paul, Brasil, 2010.
20. Dutra, C. C. G.; Trabalho de Conclusão de Curso, Universidade Federal do Rio de Janeiro, Brasil, 2019.
21. Santos, P. V. M.; Masters Dissertation, Universidade Federal do Rio Grande do Norte, Brasil, 2019.
22. Almeida, B. N.; Trabalho de Conclusão de Curso, Universidade Federal do Maranhão, Brasil, 2019.
23. Almeida, A. S.; Souza, J. G.; Madeiro, L. C. N.; Costa, M. L. A.; Cunha, A. L.; Rodrigues, M. A.; Santos, A. F.; Diversitas Journal (2019), doi: 10.17648/diversitas-journal-v4i2.593.
24. Rodrigues, T.; Masters Dissertation, Universidade Estadual do Oeste do Paraná, Brasil, 2016.
25. https://www.agencia.cnptia.embrapa.br/Repositorio/bio3_000g7gq9ghm02wx5ok0wtedt3n4jlb3w.pdf, accessed in June 2021.
26. Brown, T. L.; Lemay, E.; Burnten, B.; *Química: A ciência central*, 13ª ed., Pearson Education do Brasil Ltda: São Paulo, 2016.
27. Gentil, V.; *Corrosão*. Rio de Janeiro: LTC, 9ª ed, 2014.
28. Fernandes, D, M.; Squissato, A. L.; Lima, A. F.; Richter, E. M.; Munoz, R. A. A.; *Renewable Energy* **2019**, *139*, 1263.
29. Dahlke, T.; Ruffiner, O.; Cant, R.; *Procedia Eng.* **2016**, *138*, 231.
30. Pinto, C. F.; Antonelli, R.; de Araújo, K. S.; Fornazari, A. L. T.; Fernandes, D. M.; Granato, A. C.; Azevedo, E. B.; Malpass, G. R. P.; *Environ. Technol.* **2019**, *40*, 430.
31. Frankel, G. S.; Samaniego, A.; Birbilis, N.; *Corros. Sci.* **2013**, *70*, 104.
32. Yang, Y.; Scenini, F.; Curioni, M.; *Electrochim. Acta* **2016**, *198*, 174.
33. Pletcher, D.; Walsh, F. C.; *Industrial Electrochemistry*, 2nd ed., Springer: New York, 1993.
34. Li, P.; Chen, Y.; Li, X.; Yan, B.; Chen, D.; Guo, H.; *Int. J. Hydrogen Energy* **2020**, *45*, 17140-17152.
35. Michiels, K.; Haesen, A.; Meynen, V.; Spooren, J.; *J. Cleaner Prod.* **2018**, *195*, 674e686.
36. Song, Y.; Wightman, E.; Kulandaivelu, J.; Bu, H.; Wang, Z.; Yuan, Z.; Jiang, G.; *Water Res.* **2020**, *182*, 115961.
37. Pinto, C. F.; Masters Dissertation, Universidade Federal do Triângulo Mineiro Brasil, 2019.